[논 문] 한국재료학회지
Kor. J. Mater. Res.
Vol. 20, No. 3 (2010)

DOI: 10.3740/MRSK.2010.20.3.137

Electrical Transport Properties and Magnetoresistance of $(1-x)La_{0.7}Sr_{0.3}MnO_3/xZnFe_2O_4$ Composites

Yong Jun Seo, Geun Woo Kim, Chang Hoon Sung, Chan Gyu Lee and Bon Heun Koo†

School of Nano & Advanced Materials Engineering, Changwon National University, Changwon, Korea

(Received January 25, 2010 : Received in revised form March 3, 2010 : Accepted March 4, 2010)

Abstract The $(1-x)La_{0.7}Sr_{0.3}MnO_3$(LSMO)/$xZnFe_2O_4$(ZFO) ($x$ = 0, 0.01, 0.03, 0.06 and 0.09) composites were prepared by a conventional solid-state reaction method. We investigated the structural properties, magnetic properties and electrical transport properties of $(1-x)$LSMO/xZFO composites using X-ray diffraction (XRD), scanning electron microscopy (SEM), field-cooled dc magnetization and magnetoresistance (MR) measurements. The XRD and SEM results indicate that LSMO and ZFO coexist in the composites and the ZFO mostly segregates at the grain boundaries of LSMO, which agreed well with the results of the magnetic measurements. The resistivity of the samples increased by the increase of the ZFO doping level. A clear metal-to-insulator (M-I) transition was observed at 360K in pure LSMO. The introduction of ZFO further downshifted the transition temperature (350K-160K) while the transition disappeared in the sample (x = 0.09) and it presented insulating/semiconducting behavior in the measured temperature range (100K to 400K). The MR was measured in the presence of the 10kOe field. Compared with pure LSMO, the enhancement of low-field magnetoresistance (LFMR) was observed in the composites. It was clearly observed that the magnetoresistance effect of x = 0.03 was enhanced at room temperature range. These phenomena can be explained using the double-exchange (DE) mechanism, the grain boundary effect and the intrinsic transport properties together.

Key words $(1-x)La_{0.7}Sr_{0.3}MnO_3/xZnFe_2O_4$ (LSMO/ZFO), Low field magnetoresistance (LFMR), Curie temperature (T_c), T_{MI}.

1. Introduction

It is well known that large magnetoresistance (MR) effect of single crystals and epitaxial films of hole-doped manganite perovskites commonly occurs in the vicinity of the Curie temperature (T_C) and under a high magnetic field.[1,2] Researches[3-5] showed that the existence of grain boundaries and interfaces in manganite polycrystallines facilitates the so-called low-field magnetoresistance (LFMR), which is attributed to the spin-polarized intergrain tunneling or spin-dependent scattering at the interfaces.

Perovskite manganites with the general formula of $A_{1-x}B_xMnO_3$ (where A is lanthanum (La) element and B is an alkaline-earth (Ba, Ca, Sr) element), have attracted great attention due to the colossal magnetoresistance (CMR) effect.[6-8] Among these materials, $La_{1-x}Sr_xMnO_3$ group ($La_{0.7}Sr_{0.3}MnO_3$, $La_{2/3}Sr_{1/3}MnO_3$) has been studied intensively because of their high Curie temperature. Recently, manganite-based inorganic composites such as $La_{0.7}Sr_{0.3}MnO_3/CeO_2$, $La_{0.7}Ca_{0.3}MnO_3/SrTiO_3$, $La_{0.7}Sr_{0.3}MnO_3$ /glass, $La_{0.7}Sr_{0.3}MnO_3/CoFe_2O_4$ and $La_{0.7}Ca_{0.3}MnO_3$/ polymer composites were also investigated in Refs.[9-13]

The barrier layer for electron tunneling can be adjusted by introducing an insulating phase into the manganite to enhance the LFMR effect.[13] However, the barrier effect that the reports mentioned above is not so complete. In this paper, $ZnFe_2O_4$ is introduced to prepare $La_{0.7}Sr_{0.3}MnO_3$/ $ZnFe_2O_4$ composite. Among magnetic materials, spinel-type ferrites have gained prodigious importance.[15] As is well known, zinc ferrite ($ZnFe_2O_4$) is an antiferromagnetic normal spinel with Zn^{2+} tetrahedrally coordinated by oxygens and Fe^{3+} having an octahedral surrounding. Several groups reported that the magnetic properties of $ZnFe_2O_4$ were controlled by the super-exchange interactions introduced to modification of the distribution of Zn^{2+} and Fe^{3+} ions,[16-18] and some reports[19,20] concluded that inclusion of nonmagnetic zinc ions and the resulting magnetic disorder can be the possible causes. The MR and LFMR properties of $La_{0.7}Sr_{0.3}MnO_3/ZnFe_2O_4$ have put uncertain impacts on the development of new ferrite functional materials.[15]

In this paper, we prepared $La_{0.7}Sr_{0.3}MnO_3/ZnFe_2O_4$ composites and further investigated their magnetic and

†Corresponding author
E-Mail : bhkoo@changwon.ac.kr (B. H. Koo)

electrical transport properties. Besides, the microstructures of $ZnFe_2O_4$ and $La_{0.7}Sr_{0.3}MnO_3$ were observed. The effect of Zn-Fe_2O_4 addition on the resistivity, Curie temperature and magnetization was also evaluated. Significant enhancement in MR over a wide temperature range is observed, and the mechanism of the enhancement is also discussed.

2. Experimental Procedure

The (1-x)$La_{0.7}$ $Sr_{0.3}$ MnO_3/$x$$ZnFe_2O_4$ (LSMO/ZFO) samples (x = 0~0.09) were prepared as following steps. Firstly, the pure polycrystalline LSMO was prepared by the traditional ceramic reaction method. The stoichiometric amount of La_2O_3, Sr_2O_3 and Mn_2O_3 (the purity is higher than 99%) were ground completely to achieve the homogeneity of the mixed powder for 12h by using a ball milling and then pre-calcinated in air at 1000°C for 12h. The pre-calcinated materials were ground for 12h and pre-sintered at 1200°C for 24h. Secondly the prepared LSMO powder was mixed with $ZnFe_2O_4$ (99.9% from Aldrich) and then the mixed LSMO/ZFO powders were re-processed, according to the above experimental system to get the expected composites powder, where LSMO/ZFO is (1-x)$La_{0.7}$ $Sr_{0.3}$ MnO_3/$x$$ZnFe_2O_4$. Finally, the LSMO/ZFO composites were ground to fine powder, pressed into pellet form, and sintered at 1300°C for 24h followed by slow cooling, as is an essential and important process to favor the required oxygen content in the material. The structural properties of the LSMO/ZFO composites were analyzed by X-ray diffraction (Cu Kα_1, λ = 0.154 nm) and the scans were performed with 0.02°θ step size in the 2θ range of 20-80°. The surface morphologies of the LSMO/ZFO composites were checked by JSM 5610 scanning electron microscope. The M-T curve and resistance (Ω) were measured by using a Quantum Design Physical Properties Measurement System (PPMS) over a temperature range of 100~400K.

3. Results and Discussion

The XRD patterns of (1-x)LSMO/xZFO (x = 0~0.09) composite at room temperature are shown in Fig. 1. A rhombohedral perovskite LSMO phase and a cubic inverse spinel ZFO phase can be found in the XRD patterns. No third phase was found as the reactions

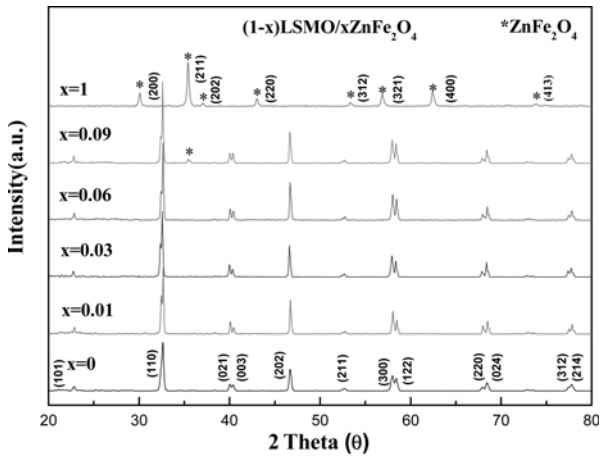

Fig. 1. X-ray diffraction patterns of (1-x)$La_{0.7}$ $Sr_{0.3}$ MnO_3/$x$$ZnFe_2O_4$ composites.

between LSMO and ZFO. The patterns also reveal that LSMO and ZFO present different types of peaks corresponding to each other. With the observation of the XRD peaks, intensity of ZFO phase gradually increases with increasing x, and no additional peaks of other phases are indicated. Consequently, it is supposed that the perovskite LSMO and the cubic inverse spinel ZFO mixed and combined well in the homogeneous granular system.

To confirm the coexistence of both phases in the composites, the LSMO/ZFO samples with the different composition of x were observed by SEM photographs. The variation of surface morphology of the LSMO/ZFO composites with ZFO(x) composition dependence is shown in Fig. 2, where two different types of crystallites can be clearly indicated. From the backscattering image of pure LSMO in Fig. 2, it is clearly seen that only LSMO phase exists. While for the composites, it is evident that the ZFO appeared as secondary phases grains located between LSMO grains. The two crystallization phases of LSMO and ZFO are clearly distinguishable from each other to form two kinds of grain boundaries labeled as LSMO/LSMO and LSMO/ZFO/LSMO. With increasing x from 0 to 0.09, the LSMO phase presents hexagonal in shape and the ZFO particles distributed uniformly among the LSMO phases, while the grain sizes of LSMO phase decreased and the content of ZFO second phase increased.

The temperature dependence of magnetization of the LSMO/ZFO composites with different composition at an applied magnetic field of 5kOe is shown in Fig. 3. All the samples present the transition from the para-

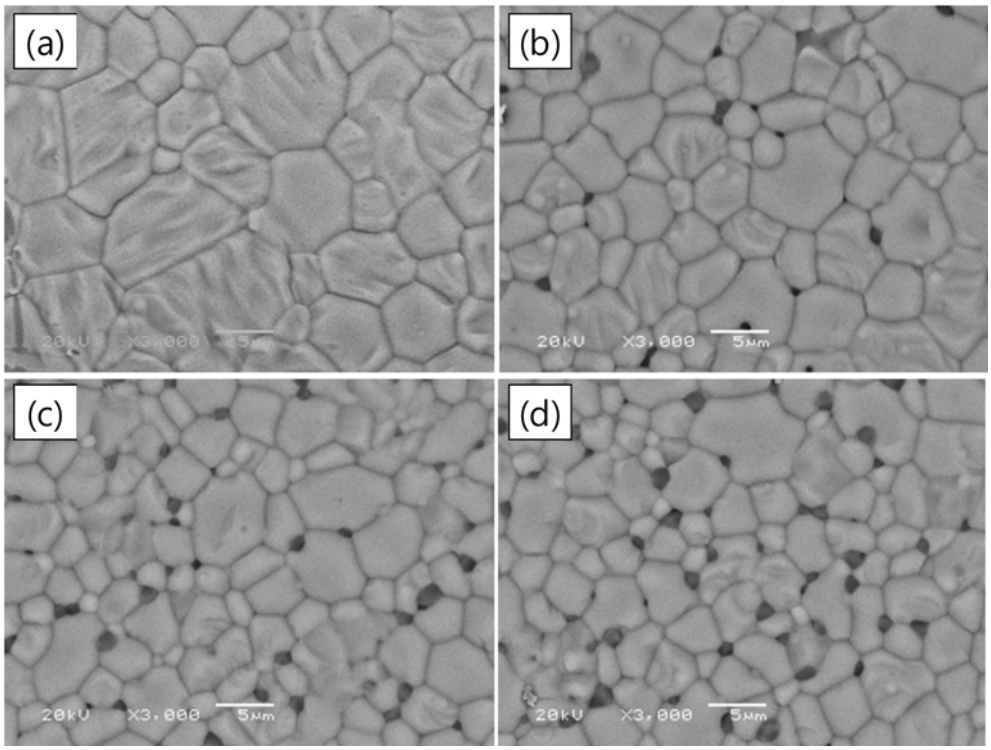

Fig. 2. SEM micrographs of (1-x)$La_{0.7}$ $Sr_{0.3}$ MnO_3/$x$$ZnFe_2O_4$ composites. (a) x = 0, (b) x = 0.01, (c) x = 0.03 and (d) x = 0.09.

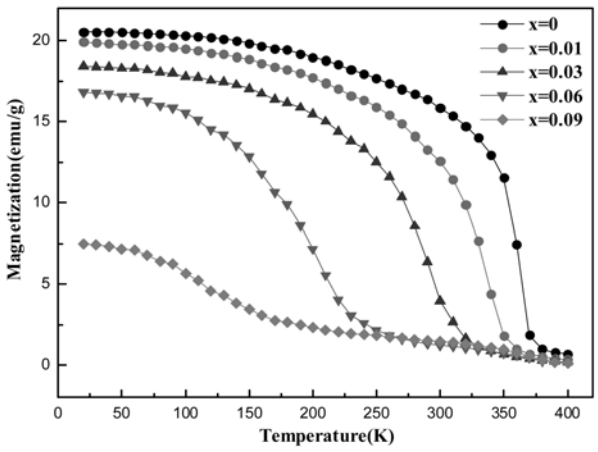

Fig. 3. Temperature dependence of Magnetization of (1-x)$La_{0.7}$ $Sr_{0.3}$ MnO_3/$x$$ZnFe_2O_4$ composites under magnetic field cooled (FC) mode (H=10kOe).

agnetic (PM) to ferromagnetic (FM). In an applied magnetic field of H_{dc}= 5kOe, when the percentage of ZFO increased from 0 to 0.09, the PM-FM transition temperature (T_c) decreased from 366.5K to 176.3K. The values of magnetization (M) at 50K are 20.5, 19.7, 18.3, 16.6 and 7.3 emu/gm, respectively. The structural and physical properties of the LSMO/ZFO composites are affected by many factors, such as the ZFO concentration. During the process, ZFO segregated into the LSMO grain boundaries and imbedded into the LSMO grains. Therefore, the segregation and the imbedded of ZFO would generate a double exchange (DE) mechanism. These segregation and imbedded effects can be well explained by FM domains walls.[21] The mentioned DE mechanism consequently results in the suppression of PM-FM transition temperature reducing towards a relative lower value as increasing ZFO concentration. The reduction in the magnetization will result in the suppression of DE mechanism to suppress the ferromagnetic alignment of Mn ions. This phenomenon also will cause the magnetic spin disorder induced by the grain boundaries in the combined system. There is a large difference between the value of metal-insulator (M-I) transition temperature (T_P) and paramagnetic-ferromagnetic transition temperature (T_c) for the combined samples. The similar movement was observed in LSMO/ $BaFe_{11.3}(ZnSn)_{0.7}O_{19}$ composites.[22]

With the temperature from 100K to 400K, the temperature dependence of resistivity in magnetic field of 0 and 10kOe is shown in Fig. 4. The value of resistivity at 100K increases from 0.004 to 5793 Ωcm^{-1} when x increase from 0 to 0.09. Meanwhile, the samples, with x = 0, 0.01, 0.03 and 0.06, show the M-I transition when

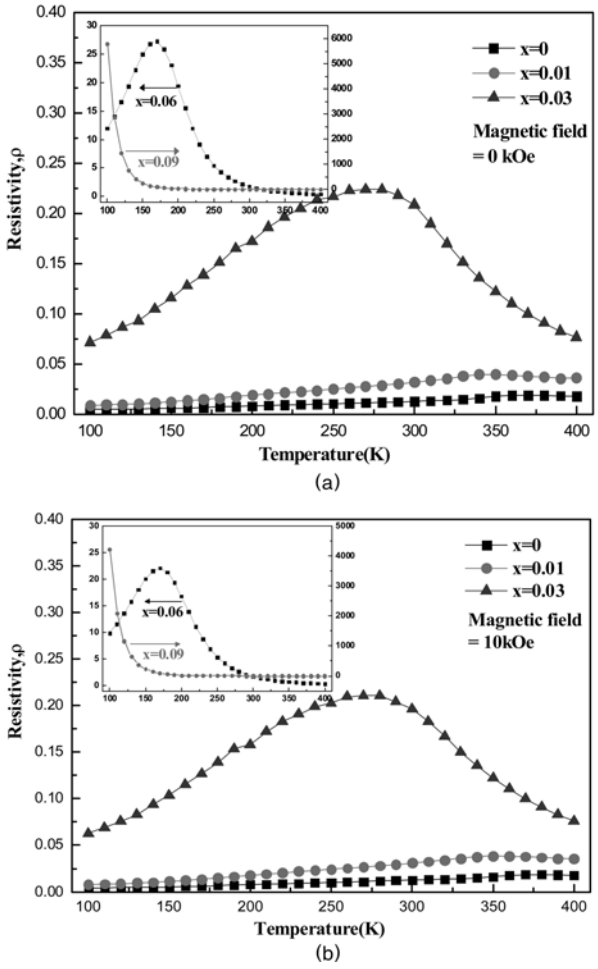

Fig. 4. Temperature dependence of resistivity in (a) magnetic field (H_{dc} = 0kOe) and (b) magnetic field (H_{dc} = 10kOe) for (1-*x*) $La_{0.7}Sr_{0.3}MnO_3$/*x*$ZnFe_2O_4$ composites.

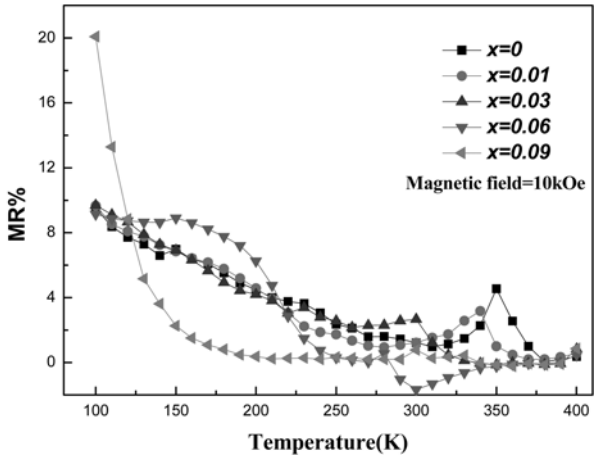

Fig. 5. Temperature dependence of magnetoresistance (MR%) under a magnetic field of H_{dc} = 10kOe for (1-*x*)$La_{0.7}Sr_{0.3}MnO_3$/*x* $ZnFe_2O_4$ composites.

the temperature increased from 360 to 140K. The transition disappears in the sample (x = 0.09) and it presents the insulating/semiconducting behaviour in the whole temperature range (100K to 400K). It is concluded that the inverse spinel $ZnFe_2O_4$ secondary phase with insulating behavior plays a negative role in the electron transport. It is generally considered that the increase of resistivity and disappearance of M-I transition are resulted by the enhanced secondary grain boundaries.[23] As a paramagnetic insulator ZFO behaves, the LSMO/ZFO samples are similar to the ferromagnet/insulator type composites. As discussed in the literature,[24] there are two kinds of conduction channels connected to the polycrystalline LSMO/ZFO composites in parallel otherwise only one channel can be directly contacted between LSMO grains, and the other related to ZFO grains. While the electrical transports are totally achieved by direct contacts between each LSMO grains in pure LSMO samples.

Fig. 5 reveals the temperature dependence of magnetoresistance (MR%) at magnetic field of H_{dc} = 10kOe of LSMO/ZFO composites with different ZFO concentration, measured over a temperature range of 100 to 400K. MR% is defined as $MR = [\rho_{(0)} - \rho_{(H)}]/\rho_{(0)}$, where $\rho_{(H)}$ and $\rho_{(0)}$ are the resistivity of the sample in and out of the external applied magnetic field. It is found that the maximum MR value of pure LSMO reached 4.8% around T_c (~350K). By application of an external magnetic field, Mn spins within the disordered regions realigned along the field direction, as a result, it enhances electron-tunneling rates between LSMO grains, and thus MR was improved. Meanwhile, the maximum MR value of the LSMO/ZFO composites is not concerned with T_c. The composition x = 0.03 shows the enhanced MR peak at 300K. When x increased over 0.03, the LFMR effect slightly decreased, as shown in Fig. 5. This phenomenon was studied by Tian,[25] where the existence of secondary phases were generated to the controlled spin-polarized intergrain tunneling effect, which was utilized by magnetic disorder at LSMO grain boundaries. Therefore, affected by the enhanced magnetic disorder, the magnetic reaction such as spin-polarized and tunneling effects are also strengthened at low external applied magnetic field.

4. Conclusions

We have studied the electrical and magnetic properties

of the (1-x)$La_{0.7}$ $Sr_{0.3}$ MnO_3/$x$$ZnFe_2O_4$ composites system. The XRD results indicated that LSMO and ZFO have different types of peaks corresponding to each other in LSMO/ZFO composite samples. There are two kinds of grain boundaries labeled as LSMO/LSMO and LSMO/ZFO/LSMO. The ZFO addition induces an increase of resistivity and a decrease of Curie temperature and magnetization. Compared with pure LSMO, the magnetoresistance property of LSMO/ZFO composites (x = 0.03) can be significantly improved.

Acknowledgement

This work was supported by the Korea Research Foundation (KRF) grant funded by the Korean Government (MEST) (No.2009-0077268). This research was supported by the MKE (The Ministry of Knowledge Economy), Korea, under the ITRC (Information Technology Research Center) support program supervised by the NIPA (National IT Industry Promotion Agency) (NIPA-2010-C1090-1021-0015).

References

1. G. C. Xiong, Q. Li, H. L. Ju, R. L. Greene and T. Venkatesan, Appl. Phys. Lett., **66**, 1689 (1995).
2. S. Jin, T. H. Tiefel, M. McCormack, R. A. Fastnacht, R. Ramesh and L. H. Chen, Science, **264**, 413 (1994).
3. X. W. Li, A. Gupta, G. Xiao and G. Q. Gong, Appl. Phys. Lett., **71**, 1124 (1997).
4. H. Y. Hwang, S.W. Cheong, N. P. Ong and B. Batlogg, Phys. Rev. Lett., **77**, 2041 (1996).
5. R. Mahesh, R. Mahendiran, A. K. Raychaudhuri and C. N. R. Rao, Appl. Phys. Lett., **68**, 2291 (1996).
6. S. Jin, T. H. Tiefel, M. McCormack, R. A. Fastnacht, R. Ramesh and L. H. Chen, Science, **264**, 413 (1994).
7. M. J. Casanove, C. Roucau, P. Baules, J. Majimel, J. C. Ousset, D. Magnoux and J. F. Bobo, Appl. Surf. Sci., **188**, 19 (2002).
8. G. B. Jeon, B. H. Koo and C. G. Lee, Kor. J. Mater. Res., **16**, 44 (2006).
9. L. Balcells, A. E. Carrillo, B. Martínez and J. Fontcuberta, Appl. Phys. Lett., **74**, 4014 (1999).
10. D. K. Petrov, L. Krusin-Elbaum, J. Z. Sun, C. Field and P. R. Duncombe, Appl. Phys. Lett., **75**, 995 (1999).
11. S. Gupta, R. Ranjit, C. Mitra, P. Raychaudhuri and R. Pinto, Appl. Phys. Lett., **78**, 362 (2001).
12. C. H. Yan, Z. G. Xu, T. Zhu, Z. M. Wang, F. X. Cheng, Y. H. Huang and C. S. Liao, J. Appl. Phys., **87**, 5588 (2000).
13. Y. H. Huang, X. Chen, Z. M. Wang, C. S. Liao, C. H. Yan, H. W. Zhao and B. G. Shen, J. Appl. Phys., **91**, 7733 (2002).
14. Y. H. Huang, S. Wang, F. Luo, S. Jiang and C. H. Yan, Chem. Phys. Lett., **362**, 114 (2002).
15. X. Bo, G. Li, X. Q. Qiu, Y. F. Xue and L. Li, J. Solid State Chem., **3**, 1038 (2007).
16. J. A. Toledo-Antonio, N. Nava, M. Martinez and X. Bokhimi, Appl. Catal., A**234**, 137 (2002).
17. G. F. Goya, H. R. Rechenberg, M. Chen and W. B. Yelon, J. Appl. Phys., **87**, 8005 (2000).
18. Z. H. Zhou, J. M. Xue, H. S. O. Chan and J. Wang, J. Appl. Phys., **90**, 4169 (2001).
19. J. F. Hochepied, P. Bonville and M. P. Pileni, J. Phys. Chem., B**104**, 905 (2000).
20. J. F. Hochepied and M. P. Pileni, J. Appl. Phys., **87**, 2472 (2000).
21. C. H. Yan, Y. H. Huang, X. Chen, C. S. Liao, Z. M. Wang, J. Phys.: Condens. Matter., **14**, 9607 (2002).
22. Q. Huang, J. Li, X. J. Huang, X. S. Gao and C. K. Ong, J. Appl. Phys., **90**, 2924 (2001).
23. A. Gaur, G. D. Varma, J. Alloy. Comp., **453**, 423 (2008).
24. M. Rubinstein, J. Appl. Phys., **87**, 5019 (2000).
25. Z. M. Tian, S. L. Yuan, Y. Q. Wang, L. Liu, S. Y. Yin, P. Li, K. L. Liu, J. H. He and J. Q. Li, Mater. Sci. Eng. B, **150**, 50 (2008).